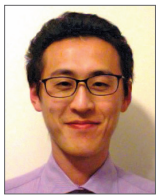


Transcatheter non-contact microwave ablation may enable circumferential renal artery denervation while sparing the vessel intima and media



Pierre C. Qian^{1,2,3*}, MBBS; Michael A. Barry^{1,4}, BSc; Sara Al-Raisi^{1,2}, MB, BCh, BAO; Pramesh Kovoor^{1,2}, MBBS, PhD; Jim Pouliopoulos^{1,2}, BSc, MSc (Med), PhD; Chrisan J. Nalliah¹, MBBS; Abhishek Bhaskaran^{1,2}, MBBS; William Chik^{1,2}, MBBS, PhD; Rahul Kurup¹, MBBS; Virginia James³, MSc; Winny Varikatt⁵, MBBS, PhD; Alistair McEwan^{1,4}, BEng, MEng, PhD, S.M.I.E.E.; Aravinda Thiagalingam^{1,2,3}, MB, ChB, PhD; Stuart P. Thomas^{1,2,3}, MBBS, PhD

1. Cardiology Department, Westmead Hospital, Sydney, Australia; 2. Sydney Medical School, University of Sydney, Sydney, Australia; 3. The Westmead Institute for Medical Research, Sydney, Australia; 4. School of Electrical and Information Engineering, University of Sydney, Sydney, Australia; 5. Anatomical Pathology Laboratory, Institute of Clinical Pathology and Medical Research, Westmead Hospital, Sydney, Australia

KEYWORDS

- catheter ablation
- innovation
- preclinical research
- renal sympathetic denervation

Abstract

Aims: Trials of transcatheter renal artery denervation (RDN) have failed to show consistent antihypertensive efficacy. Procedural factors and limitations of radiofrequency ablation can lead to incomplete denervation. The aim of the study was to show that non-contact microwave catheter ablation could produce deep circumferential perivascular heating while avoiding injury to the renal artery intima and media.

Methods and results: A novel microwave catheter was designed and tested in a renal artery model consisting of layers of phantom materials embedded with a thermochromic liquid crystal sheet, colour range 50-78°C. Ablations were performed at 140 W for 180 sec and 120 W for 210 sec, delivering 25,200 J with renal arterial flow at 0.5 L/min and 0.1 L/min. Transcatheter microwave ablations 100-160 W for 180 sec were then performed in the renal arteries of five sheep. *In vitro*, ablations at 140 W and 0.5 L/min flow produced circumferential lesions 5.9±0.2 mm deep and 19.2±1.5 mm long with subendothelial sparing depth of 1.0±0.1 mm. *In vivo*, transcatheter microwave ablation was feasible with no collateral visceral thermal injury. There was histological evidence of preferential outer media and adventitial ablation.

Conclusions: Transcatheter microwave ablation for RDN appears feasible and provides a heating pattern that may enable more complete denervation while sparing the renal arterial intima and media.

*Corresponding author: Department of Cardiology, Westmead Hospital, Cnr of Hawkesbury and Darcy Rd, Westmead, Sydney, NSW 2145, Australia. E-mail: pierre.qian@sydney.edu.au

Abbreviations

NBT	nitroblue tetrazolium
RDN	renal artery denervation

Introduction

Hypertension is a global health crisis, affecting one in three adults causing death and disability from cardiovascular disease^{1,2}. In a Western population, up to one in eight patients fail to achieve adequate blood pressure control despite the use of three antihypertensive agents and are termed to have resistant hypertension³. Renal efferent and afferent nerve hyperactivity in this patient group has been implicated as a major driver of hypertension, causing salt and fluid retention and increased vascular tone and heart rate⁴. Initially, in small clinical trials, transcatheter renal artery denervation (RDN) appeared safe and efficacious⁵. However, SYMPPLICITY HTN-3, the largest randomised clinical trial for transcatheter RDN, failed to show blood pressure reduction against a sham control.

Radiofrequency energy has inherently limited depth of heating and ability to provide circumferential renal nerve ablation, which could contribute to incomplete denervation and inconsistent clinical efficacy. Radiofrequency heating is ohmic and directly heats only a small region at the catheter tissue interface. The majority of lesion growth is driven by thermal conduction from this zone into the surrounding tissue⁶. Radiofrequency denervation systems must down-modulate power during ablation to avoid excessive catheter tissue interface heating and consequent vascular injury or thrombosis; this limits the average lesion depth to 2–4 mm^{7,8}. Fixed perfused human cadaveric studies suggest that a 2 mm lesion depth could reach 30–50% of renal nerves and 4 mm lesion depth could reach 60–80%; yet, in order to reach at least 90% of renal nerves consistently, a depth of approximately 6 mm would be required⁹. As radiofrequency ablation causes transmural injury to the renal artery, a discontinuous spiral configuration of ablation lesion is necessary to avoid renal artery stenosis. The success of such a strategy depends on a parallel course of renal nerves. Instead, renal nerves in humans probably form an arborising plexus as nerve bundle counts differ between proximal, mid and distal renal artery segments⁹, giving rise to the possibility that such a set of focal lesions may be bypassed by the nerve network. Indeed, norepinephrine spillover measurements following radiofrequency RDN show inconsistent and incomplete levels of denervation¹⁰. Furthermore, recent animal studies of RDN using radiofrequency ablation have shown evidence of neuroregeneration at the site of focal ablation and full recovery of afferent and efferent renal nerve function by 5.5 months, indicating that denervation is not sustained^{11,12}.

Microwave energy has properties that are highly suited for RDN. Microwave heating is dielectric and not contact-dependent, making it possible to heat deeper tissues directly while simultaneously avoiding high temperatures in the renal artery wall, which is cooled by adjacent blood flow^{13,14}. We hypothesised that a microwave catheter centred in a renal artery could create a thermal lesion that is: (i) circumferential around the renal artery, and (ii) deeper than

radiofrequency ablation with the potential to encompass the majority of renal nerves; while (iii) avoiding thermal injury to a subendothelial zone thick enough to spare the renal artery intima and media. Using phantom renal artery models, we determined the heating pattern produced by transcatheter microwave ablation and investigated the effects of renal artery flow and microwave energy delivery rate on thermal lesion dimensions. Subsequently, we performed transcatheter microwave ablation in a sheep model to demonstrate procedural feasibility for RDN and provide preliminary observations on the immediate histological effects of microwave heating.

Methods

MICROWAVE ABLATION SYSTEM

An open irrigated 7 Fr microwave ablation catheter was designed and manually assembled. It consisted of a coaxial cable terminating as a side-firing microwave radiator housed in an outer sheath with an inbuilt centring mechanism. Room temperature saline was infused between the outer sheath and the coaxial cable during ablation via a CoolFlow[®] pump (Biosense Webster, Inc., Diamond Bar, CA, USA) at 35 mL/min. The catheter radiating element length was optimised to provide good microwave coupling to the renal artery model environment, with a standing wave ratio of 1.20, corresponding to a radiating efficiency of more than 99%. During *in vitro* testing with ablation power up to 140 W and renal artery flow as low as 0.1 L/min, the temperature of the saline around the radiating element rose no more than approximately 1°C irrespective of catheter irrigation, measured using Fluoroptic[®] thermometry with Luxtron probes (Model 3100; Luxtron Corp., now LumaSense Technologies, Inc., Santa Clara, CA, USA). Microwave power was supplied by a 2.45 GHz microwave generator (S250; Astex, now MKS Instruments, Inc., Wilmington, MA, USA). Power was measured using two Agilent V3500 power meters (Agilent Technologies, Santa Clara, CA, USA) connected to an eMeca 722–40–3.100 40 dB dual directional coupler (MECA Electronics Inc., Denville, NJ, USA).

LONGITUDINAL PHANTOM MODEL OF THE RENAL ARTERY

A longitudinal model of a 5 mm diameter renal artery was constructed using concentric layers of transparent phantom materials with similar microwave absorption, heating and heat conduction properties to their respective tissues. A 3 mm thick microwave muscle equivalent phantom layer consisting of 70% 0.9% saline and 30% glycerol mixed volume per volume as described previously¹⁵ solidified with 1% weight per volume gellan (Phytigel[™]; Sigma-Aldrich Corporation, St Louis, MO, USA) substituted the renal artery wall and inner nerve layers. A 10 mm thick poly(methyl-methacrylate) layer (permittivity=3.15, specific heat capacity=1.38 kJ/kg°C and thermal conductivity=0.19 W/m°C)¹⁶ substituted the perinephric fat layer (fat permittivity=5.5, specific heat capacity=1.67 kJ/kg°C and thermal conductivity=0.18 W/m°C)^{17,18}. Another layer of muscle equivalent phantom, peripheral to the perinephric fat, modelled potential water-rich nearby viscera. These materials were embedded with a custom

thermochromic liquid crystal sheet that displayed a gradual transition in colours for temperatures between 50°C and 78°C. This technique of isothermal mapping has been validated previously and can determine phantom material temperatures with a standard error of 0.5°C¹⁹; 37°C 0.9% saline was perfused through the renal artery model with flow measured using a Dwyer RMB-82D-SSV flow meter (Dwyer Instruments Pty Ltd, Unanderra, NSW, Australia) (Figure 1).

MICROWAVE ABLATION IN THE LONGITUDINAL PHANTOM MODEL, LESION MEASUREMENT AND STATISTICS

The microwave catheter was placed inside the modelled renal artery and centred using its own centring mechanism. Ablations were performed to deliver the same dose of energy (25,200 J of generator output) at 140 W for 180 sec and 120 W for 210 sec with

renal artery flow at 0.5 L/min and 0.1 L/min. With each power and flow setting, ablations were performed four times with at least three minutes of cooling time in between ablations. Digital photography of the thermochromic film was performed at baseline and then every 10 seconds to document lesion development. Thermal lesion boundaries were defined by the 53°C isotherm, which is the approximate temperature above which lethal hyperthermia occurs in muscle tissue²⁰, and measured with in-house built software.

The maximal lesion depth and length as well as the depth of subendothelial sparing, defined as the minimal perpendicular distance from the luminal surface to the 53°C isotherm, were measured (Figure 2). GraphPad Prism 6 (GraphPad Software Inc., La Jolla, CA, USA) was used for statistical analysis. Averaged final lesion dimensions±SD were represented to the nearest 0.1 mm, and statistical comparisons between groups were made using unpaired t-tests and considered significant for $p < 0.05$.

COMPARISON OF NON-CONTACT MICROWAVE AND RADIOFREQUENCY ABLATION TEMPERATURE DISTRIBUTION IN THE CROSS-SECTIONAL PHANTOM MODEL

A cross-sectional phantom renal artery model was used to compare the heating pattern between the Symplicity Flex™ denervation

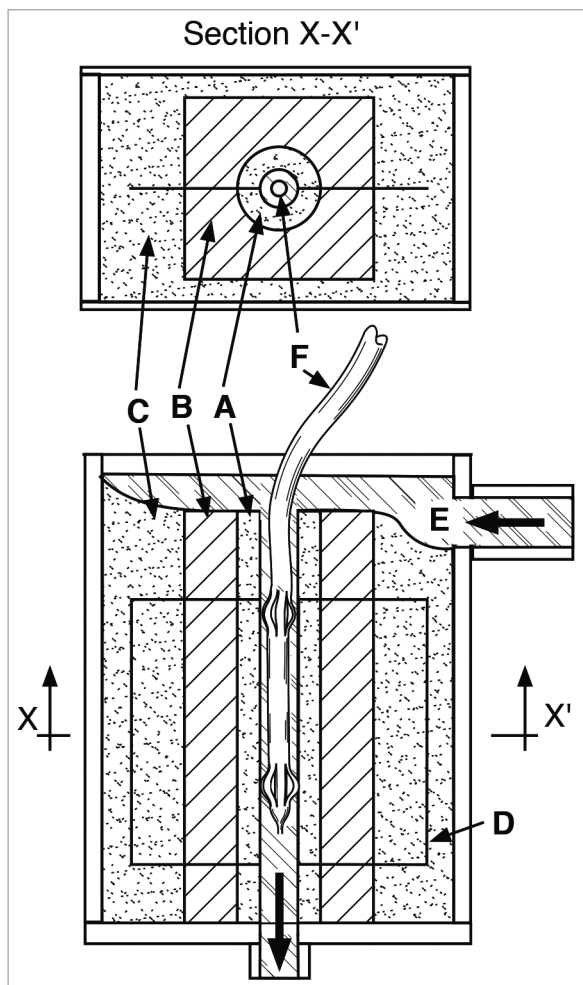


Figure 1. Longitudinal phantom renal artery denervation model. A) Renal artery and adventitial nerve layer. B) Perinephric fat layer. C) Nearby viscera layer. D) Embedded sheet of thermochromic liquid crystal with colour range 50-78°C. E) 37°C 0.9% saline solution flowing through modelled renal artery lumen. F) Prototype microwave catheter placed in the renal artery model and centred using expandable splines.

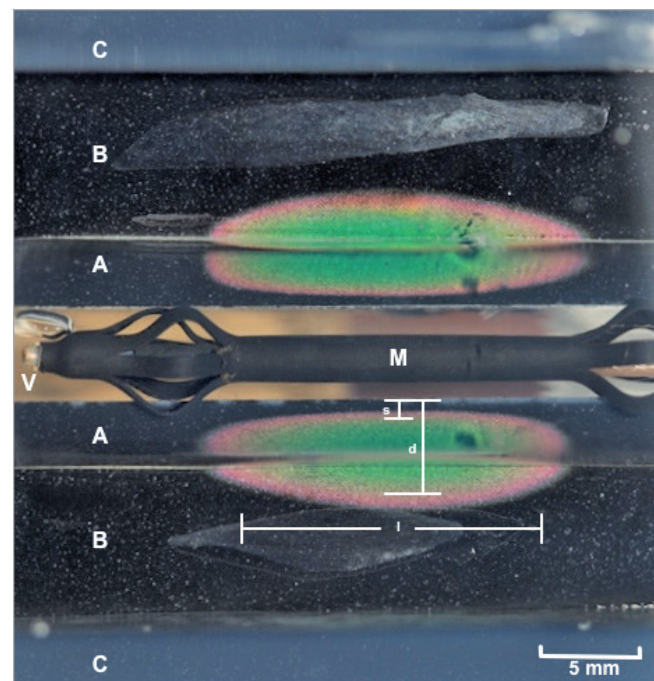


Figure 2. Thermal lesion produced by non-contact microwave ablation in the phantom model visualised on thermochromic liquid crystal sheet. A) Renal artery and adventitial nerve layer. B) Perinephric fat layer. C) Nearby viscera layer. M) Radiating element of the catheter. V) Renal artery lumen with flowing 37°C saline. Fluoroptic thermometry performed during catheter testing showed no more than 1°C rise of saline temperatures adjacent to the radiating element. d: lesion depth; l: lesion length; s: depth of subendothelial sparing

system (Medtronic, Minneapolis, MN, USA) and the prototype microwave denervation system as previously described⁷. Briefly, it consisted of a block of transparent muscle equivalent phantom gel around a 5 mm diameter 0.9% normal saline filled renal artery with flow at 0.5 L/min and temperature 37°C. For radiofrequency ablation, a radiofrequency muscle equivalent phantom composed of 30% 0.9% saline and 70% distilled water mixed volume per volume was used, as described⁷, while for microwave ablations a microwave muscle equivalent phantom composed of 70% 0.9% saline and 30% glycerol mixed volume per volume was used¹⁵; both were solidified with 1% weight per volume gellan. The gels were embedded with discs of 50-78°C temperature range thermochromic liquid crystal sheet to visualise lesion temperatures.

Radiofrequency ablation was performed at clinically recommended settings of up to 8 W for 120 sec gated at 70°C catheter tip temperature. Microwave ablation was performed at 120 W for 120 sec. Final ablation images were analysed with in-house built

software, and GraphPad Prism 6 was used to plot the lesion temperature against perpendicular depth from the luminal surface (**Figure 3**).

TRANSCATHETER MICROWAVE ABLATION IN VIVO

The study was approved by the Western Sydney Local Health District Animal Ethics Committee. Five sheep underwent transcatheter microwave ablation under general anaesthesia. An 8.5 Fr Agilis™ sheath (St. Jude Medical, St. Paul, MN, USA) was introduced via a femoral artery approach to engage the renal arteries and deliver the microwave ablation catheter under fluoroscopy (Artis zee; Siemens, Munich, Germany). One to two ablations were performed per renal artery at 100-160 W for 180 sec. Renal angiography was performed following ablations and the percentage of acute renal artery narrowing estimated visually by a cardiologist (P. Qian). The sheep were euthanised immediately post procedure to inspect for the extent of visible injury to adjacent organs and to remove the renal artery and kidneys for assessment.

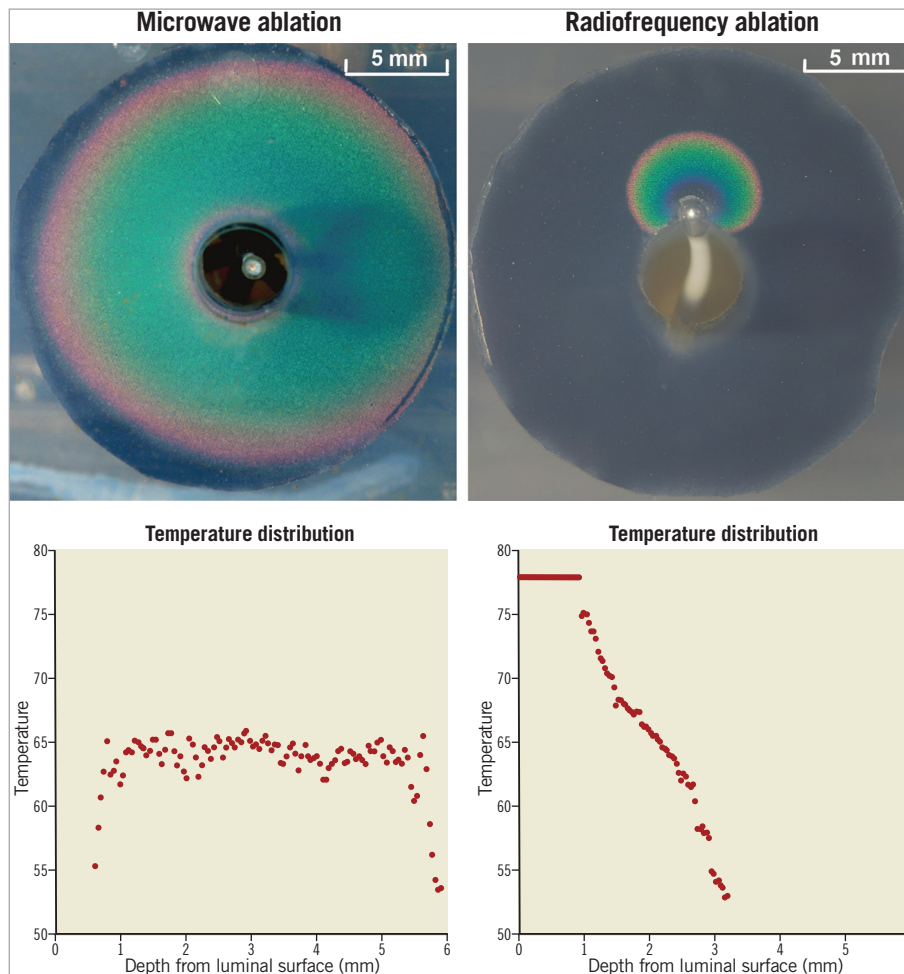


Figure 3. *In vitro* comparison of lesion temperature distribution between microwave and radiofrequency ablation. Microwave ablation performed at 120 W for 120 sec provided a more uniform thermal distribution and lower peak lesion temperature than the Symplicity Flex denervation system at standard clinical settings (up to 8 W, catheter temperature 70°C, for 120 sec). Tissue temperatures near vessel lumen were minimal with microwave ablation as compared with radiofrequency ablation which exceeded 78°C (outside the colour range of the thermochromic liquid crystal material).

For the first sheep, the perinephric fat around the renal artery was stripped before staining with nitroblue tetrazolium (NBT) for 72 hrs at 4°C. The perinephric fat was kept intact around the renal arteries in subsequent sheep. Specimens were fixed with 10% neutral buffered formalin before paraffin embedding and staining with haematoxylin and eosin.

QUANTITATIVE ANALYSIS OF NBT STAINING

Relative reductions in blue colour intensity after NBT staining inferring ablated tissue were confirmed using quantitative colorimetry. Digital photographs of the NBT-stained excised renal arteries were imported into in-house software, which was developed using MATLAB (R2014b; The MathWorks, Inc., Natick, MA, USA). Automated quantitative assessment of microwave lesions was performed using the following approach: (1) selection of the region of interest; (2) regional extraction of red, blue and green colour composites, with dimensionless values from 0 to 1, for each longitudinal segment (averaged latitudinally); (3) regional subtraction of green and red intensity values from twice the blue intensity value to obtain a relative blue intensity; (4) taking the difference between the relative blue intensities at each longitudinal position along the renal arteries with that of an unablated section to obtain a differential blue intensity. Regions with a differential blue intensity <0 thus indicated less NBT staining compared with the referenced normal tissue.

Results

MICROWAVE ABLATION HEATING PATTERN AND LESION DIMENSIONS IN THE PHANTOM RENAL ARTERY MODELS

Microwave ablation produced circumferential thermal lesions in the phantom models. Lesion growth occurred in the perivascular region and expanded towards the perinephric fat layer and the arterial lumen. Ablations at 140 W compared with 120 W at 0.5 L/min renal artery flow yielded significantly longer (19.2 ± 1.5 mm vs. 15.2 ± 2.2 mm, $p<0.001$) and deeper (5.9 ± 0.2 mm vs. 5.5 ± 0.3 mm, $p<0.03$) lesions with less subendothelial sparing (1.0 ± 0.1 mm vs. 1.2 ± 0.1 mm, $p<0.001$). At 180 sec into ablation with 0.5 L/min renal artery flow, the greater cumulative microwave dose delivered at 140 W compared with 120 W produced deeper (4.8 ± 0.3 mm vs. 4.0 ± 0.4 mm, $p<0.0002$) and longer lesions (19.2 ± 1.5 mm vs. 14.9 ± 2.3 mm, $p<0.0006$) with less subendothelial sparing (1.0 ± 0.1 mm vs. 1.2 ± 0.1 mm, $p<0.002$). At the reduced arterial flow rate of 0.1 L/min, lesion length and depth were similar

between 120 W and 140 W ablations but subendothelial sparing was reduced at the higher ablation power (0.8 ± 0.1 mm vs. 1.1 ± 0.1 mm, $p<0.0002$) (Table 1, Figure 4). The mean peak lesion temperatures were similar in high and low renal artery flow conditions at 120 W and 140 W and did not exceed approximately 68°C

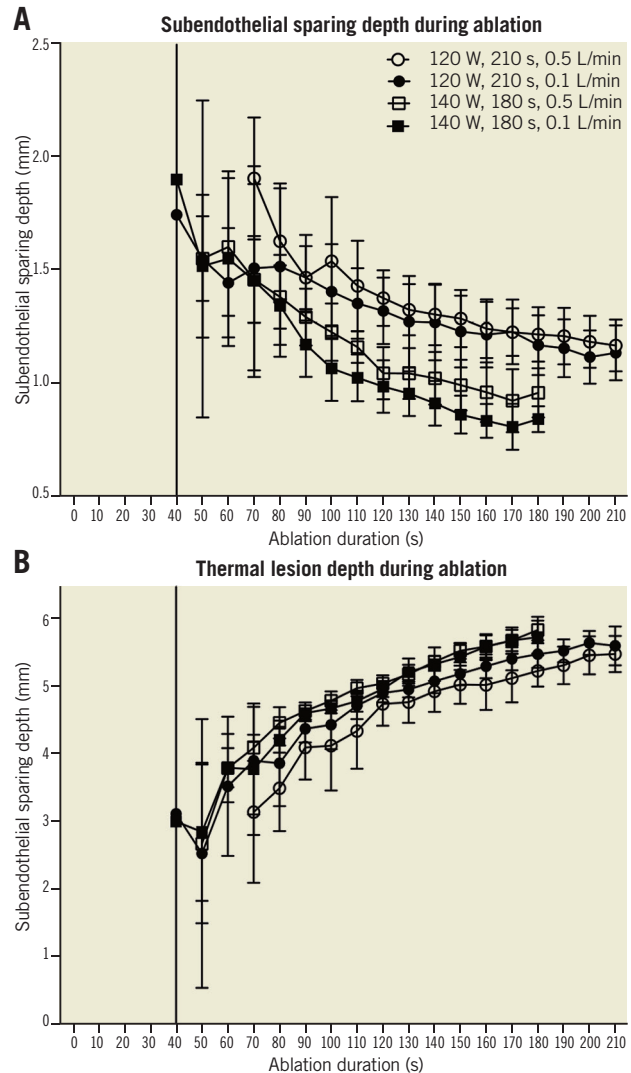


Figure 4. Microwave thermal lesion dimensions. The average depth from the lumen of the vessel that is spared from lethal heating is shown at each time point with 95% confidence intervals (A). The average lesion depth is shown at each time point during ablation with 95% confidence intervals (B).

Table 1. Final lesion characteristics at varying power and renal artery flow.

	Lesion depth (\pm SD)	Subendothelial sparing depth (\pm SD)	Lesion length (\pm SD)	Mean peak lesion temperature (\pm SD)
120 W for 210 sec at 0.5 L/min	5.5 ± 0.3 mm	1.2 ± 0.1 mm	15.2 ± 2.2 mm	$67.0\pm 0.7^\circ\text{C}$
120 W for 210 sec at 0.1 L/min	5.6 ± 0.3 mm	1.1 ± 0.1 mm	16.9 ± 1.8 mm	$66.8\pm 0.6^\circ\text{C}$
140 W for 180 sec at 0.5 L/min	5.9 ± 0.2 mm	1.0 ± 0.1 mm	19.2 ± 1.5 mm	$67.5\pm 1.0^\circ\text{C}$
140 W for 180 sec at 0.1 L/min	5.8 ± 0.3 mm	0.8 ± 0.1 mm	18.2 ± 2.0 mm	$68.1\pm 0.6^\circ\text{C}$

(Table 1). No heating peripheral to the 10 mm thick perinephric fat layer was observed in any of the ablations.

MICROWAVE AND RADIOFREQUENCY ABLATION TEMPERATURE DISTRIBUTIONS

Microwave ablations produced a zone of subendothelial sparing with temperatures peaking in the perivascular region. Radiofrequency ablation produced peak heating at the catheter tissue interface, which was beyond the 78°C upper limit of the TLC, that dropped away rapidly with depth. Microwave heating produced a more homogenous temperature distribution with lower peak lesion temperature than radiofrequency ablation. The depth of lethal hyperthermia was notably greater with microwave as compared with radiofrequency ablation at the tested ablation settings (Figure 3).

TRANSCATHETER MICROWAVE ABLATION IN SHEEP

The investigational microwave transcatheter system was deployed and ablation performed in eight of ten targeted renal arteries. Of the two renal arteries that could not be treated, one could not be found using the Agilis sheath and the other was not ablated due to technical failure of the irrigation pump; these have not been included in the analysis. Nine ablations were performed: three 160 W ablations, three 140 W ablations, two 120 W ablations and a 100 W ablation. All of these ablations were delivered to the middle portion of the renal artery except for an ablation at 140 W, which was performed in the distal renal artery at a trifurcation close to the renal hilum. Following microwave ablation, renal artery spasm was routinely observed causing <50% renal artery narrowing in eight of nine ablations (Figure 5). One ablation produced an eccentric 80% narrowing after 160 W was applied in a tortuous renal artery, but there was no histological evidence of transmural arterial injury at this site.

No gross acute injuries to nearby viscera were observed with any ablations. Histological assessment showed a notable lack of architectural disruption. Renal arterial ablation injury was seen in only four of nine ablations. Eccentric catheter position accounted for two of these, which demonstrated a region of linear transmural injury. No circumferential transmural injury was observed in any of the specimens. In each case where ablation to the renal arterial wall was seen, there were regions where a predominantly outer media and adventitial ablation had taken place with sparing of more inner layers of the vessel wall (Figure 6). When the renal artery was directly stained with NBT, circumferential ablation to the adventitial aspect of the renal arteries could be better appreciated. Again, regions of preferential adventitial ablation with sparing of the luminal aspect of the artery were seen (Figure 5). No immediate histological changes could be appreciated in the perivascular region.

Discussion

In these studies we have demonstrated that microwave energy can be used to perform a circumferential perivascular ablation with controllable lesion depth and subendothelial sparing. The potential to deliver deeper and more complete ablation of the renal nerves

while avoiding significant renal arterial injury provides important advantages over radiofrequency ablation systems. This may enable a microwave ablation system to achieve more consistent and durable denervation efficacy.

In the phantom renal artery model, non-contact transcatheter microwave ablation was capable of forming circumferential lesions 5.9 mm deep at the tested ablation settings. This depth is superior to the 3.4-3.8 mm achieved using EnligHTN™ (St. Jude Medical) and Symplicity denervation systems when tested in a similar *in vitro* preparation and sufficient to encompass approximately 90% of renal nerves circumferentially if reproduced *in vivo*^{7,9}. Also, lesion lengths *in vitro* were up to 19.2 mm from a single ablation, posing a substantial gap over which neuroregenerative responses must bridge to reinnervate. Subendothelial sparing varied between approximately 0.8 and 1.2 mm, sufficient to spare the renal arterial intima and media which is approximately 0.5 mm²¹.

Perivascular thermal lesion growth was governed by the balance between microwave heating and luminal cooling from arterial flow acting in opposition. Higher cumulative microwave energy dose increased lesion depth, and a lower rate of energy delivery (power) enabled increased subendothelial sparing. In the case of low renal artery flow, the same microwave energy load can be given over a longer duration at lower power to achieve a similar lesion depth but with significantly more subendothelial sparing (Table 1, Figure 4). The near absence of catheter tip heating with microwave ablation (only 1°C) makes it possible to use much higher powers to achieve larger volume thermal lesions compared with radiofrequency ablation, where high catheter-tissue interface temperatures limit ablation power and lesion depth (Figure 3).

In vivo study demonstrated the feasibility and acute tolerability of delivering a microwave transcatheter device transarterially and performing an ablation. The procedure appeared safe with no collateral thermal injury observed to adjacent organs despite ablations up to 160 W, as predicted *in vitro*. Cooling from renal artery flow was sufficient *in vivo* during these ablations to protect against significant arterial injury despite high ablation power. Regions of ablation in the renal artery wall involving the outer media and adventitia with subendothelial sparing could be appreciated histologically and on viability staining with NBT (Figure 5, Figure 6). Where transmural arterial ablation had occurred due to eccentric catheter position, they were linear and parallel with the artery and not expected to result in renal artery stenosis. Renal nerve injury could not be appreciated at this early time point immediately following ablation. The subtle histological changes and absence of coagulative necrosis or tissue desiccation was consistent with a low temperature thermal injury, as seen *in vitro*. Histological assessment of ablation lesions at days or weeks post procedure is required to demarcate the full extent of irreversible thermal tissue injury.

Novel denervation technologies capable of circumferential ablation such as the ultrasound-based Paradise® System (ReCor Medical, Palo Alto, CA, USA) and the injection-based Peregrine

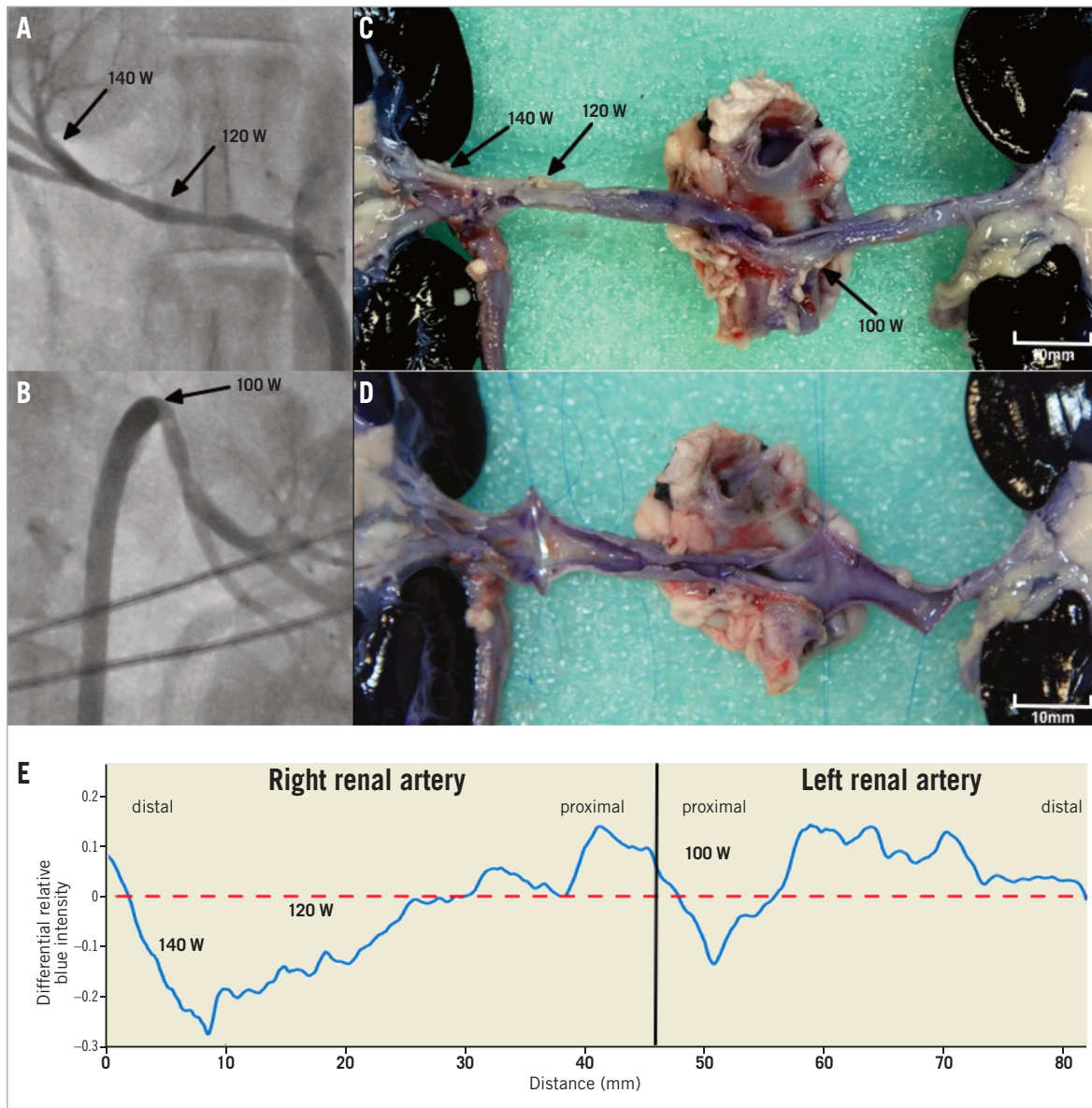


Figure 5. Gross histological changes after intravascular non-contact microwave ablation in sheep renal artery. Renal angiography of the right (A) and left (B) renal arteries after ablations at the indicated power (black arrows) for 180 sec. Nitroblue tetrazolium treatment revealed circumferential adventitial thermal injury at the site of each ablation (C). In the 140 W and 120 W ablations, inspection of the vessel lumen showed viable tissue anteriorly indicating a predominantly adventitial ablation in this region. Posteriorly, there was ablation to both the luminal and the adventitial aspect, indicating a linear transmural lesion due to eccentric catheter position. The 100 W ablation produced a predominantly adventitial ablation (D). Colorimetric analysis confirmed adventitial ablation (E).

System™ (Ablative Solutions, Kalamazoo, MI, USA) have shown capacity to produce renal denervation in preclinical studies and are the subject of ongoing clinical trials. It remains to be demonstrated that these technologies are superior to radiofrequency ablation in producing durable denervation. Microwave ablation has the theoretical advantage over these systems in terms of penetration through areas of vascular calcification. Given the different mechanism by which these novel modalities produce tissue injury, comparison of lesion formation capacity and effectiveness of subsequent neuro-regenerative responses requires long-term *in vivo* studies.

Study limitations

Microwave thermal lesion dimensions *in vitro* may not be indicative of the ablation lesions *in vivo* at the same ablation settings. However, given the potential renal artery intima and media sparing with non-contact microwave ablation *in vitro* and *in vivo*, we posit that sufficiently high energy ablations could allow deep circumferential lesions to be delivered *in vivo*. We did not determine whether the microwave ablations delivered *in vivo* led to renal denervation. Given the high microwave ablation powers used, it was necessary to establish that the procedure could be safely performed in order to plan longer-term dose-finding *in vivo* studies.

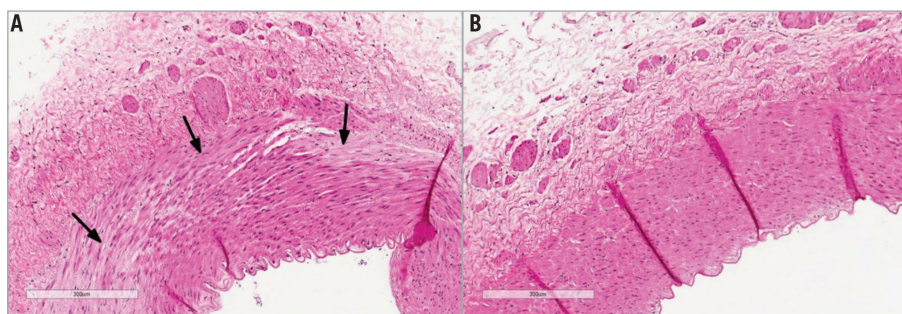


Figure 6. Early histological changes in the renal artery wall following microwave ablation. Haematoxylin and eosin stained sections through the 140 W ablation (shown in Figure 5) (A), compared with the unablated distal left renal artery as a control (B). Regional myocyte oedema and myocyte death in the outer tunica media (black arrows) as well as oedema in the overlying adventitia with relative preservation of vascular intima and the internal elastic lamina.

Conclusions

We have provided a proof of principle that microwave transcatheter ablation from within the renal artery can create deep circumferential perivascular heating while avoiding circumferential transmural arterial ablation. This heating pattern may enable more consistent and complete renal nerve ablation to be performed without significant arterial injury. We have also demonstrated the feasibility of performing transcatheter non-contact microwave RDN *in vivo*.

Impact on daily practice

The use of radiofrequency energy for RDN has inherent biophysical limitations that impact on the effectiveness and durability of therapy; these may be overcome by novel methods and energy sources. We have demonstrated the potential for microwave energy to be used for RDN and the value of using an *in vitro* phantom model for assaying and optimising novel denervation technology. Without careful preclinical evaluation, optimisation and comparison of denervation technologies to improve the potential consistency and durability of therapy, future clinical trials of RDN risk futility due to ineffective denervation.

Funding

This study was supported by the Department of Cardiology, Westmead Hospital, Sydney, and the Commercial Development & Industry Partnerships Fund (CDIP19-2015), University of Sydney. P. Qian was supported by a National Health and Medical Research Council (NHMRC) and National Heart Foundation of Australia (NHF) co-funded postgraduate scholarship (NHMRC Scholarship No. 1114408, NHF Scholarship No. 101107).

Conflict of interest statement

P. Qian and M. Barry are inventors of the patented microwave system used in this study with intellectual property rights assigned to the University of Sydney and Westmead Hospital. The other authors have no conflicts of interest to declare.

References

1. Roger VL, Go AS, Lloyd-Jones DM, Benjamin EJ, Berry JD, Borden WB, Bravata DM, Dai S, Ford ES, Fox CS, Fullerton HJ, Gillespie C, Hailpern SM, Heit JA, Howard VJ, Kissela BM, Kittner SJ, Lackland DT, Lichtman JH, Lisabeth LD, Makuc DM, Marcus GM, Marelli A, Matchar DB, Moy CS, Mozaffarian D, Mussolino ME, Nichol G, Paynter NP, Soliman EZ, Sorlie PD, Sotoodehnia N, Turan TN, Virani SS, Wong ND, Woo D, Turner MB; American Heart Association Statistics Committee and Stroke Statistics Subcommittee. Heart disease and stroke statistics-2012 update: a report from the American Heart Association. *Circulation*. 2012;125:e2-e220.
2. World Health Organization. A global brief on hypertension: silent killer, global public health crisis. Geneva, World Health Organization. 2013.
3. Persell SD. Prevalence of resistant hypertension in the United States, 2003-2008. *Hypertension*. 2011;57:1076-80.
4. Todoran TM, Basile JN, Zile MR. Renal sympathetic denervation for blood pressure control: a review of the current evidence and ongoing studies. *J Clin Hypertens*. 2014;16:331-41.
5. Kandzari DE, Bhatt DL, Sobotka PA, O'Neill WW, Esler M, Flack JM, Katzen BT, Leon MB, Massaro JM, Negoita M, Oparil S, Rocha-Singh K, Straley C, Townsend RR, Bakris G. Catheter-based renal denervation for resistant hypertension: rationale and design of the SYMPPLICITY HTN-3 trial. *Clin Cardiol*. 2012;35:528-35.
6. Haines DE. Determinants of lesion size during radiofrequency catheter ablation: the role of electrode-tissue contact pressure and duration of energy delivery. *J Cardiovasc Electrophysiol*. 1991;2:509-15.
7. Al Raisi SI, Pouliopoulos J, Barry MT, Swinnen J, Thiagalingam A, Thomas SP, Sivagangabalan G, Chow C, Chong J, Kizana E, Kovoov P. Evaluation of lesion and thermodynamic characteristics of Symplicity and EnligHTN renal denervation systems in a phantom renal artery model. *EuroIntervention*. 2014;10:277-84.
8. Mahfoud F, Edelman ER, Böhm M. Catheter-based renal denervation is no simple matter: lessons to be learned from our anatomy? *J Am Coll Cardiol*. 2014;64:644-6.

9. Sakakura K, Ladich E, Cheng Q, Otsuka F, Yahagi K, Fowler DR, Kolodgie FD, Virmani R, Joner M. Anatomic assessment of sympathetic peri-arterial renal nerves in man. *J Am Coll Cardiol*. 2014;64:635-43.
10. Esler M. Renal denervation: Not as easy as it looks. *Sci Transl Med*. 2015;7:285fs18.
11. Booth LC, Nishi EE, Yao ST, Ramchandra R, Lambert GW, Schlaich MP, May CN. Reinnervation of renal afferent and efferent nerves at 5.5 and 11 months after catheter-based radiofrequency renal denervation in sheep. *Hypertension*. 2015;65:393-400.
12. Sakakura K, Tunev S, Yahagi K, O'Brien AJ, Ladich E, Kolodgie FD, Melder RJ, Joner M, Virmani R. Comparison of histopathologic analysis following renal sympathetic denervation over multiple time points. *Circ Cardiovasc Interv*. 2015;8:e001813.
13. Thomas SP, Clout R, Deery C, Mohan AS, Ross DL. Microwave ablation of myocardial tissue: the effect of element design, tissue coupling, blood flow, power, and duration of exposure on lesion size. *J Cardiovasc Electrophysiol*. 1999;10:72-8.
14. Qian P, Barry MA, Nguyen T, Ross D, Kovoov P, McEwan A, Thomas S, Thiagalingam A. A Novel Microwave Catheter Can Perform Noncontact Circumferential Endocardial Ablation in a Model of Pulmonary Vein Isolation. *J Cardiovasc Electrophysiol*. 2015;26:799-804.
15. Lin JC. Catheter microwave ablation therapy for cardiac arrhythmias. *Bioelectromagnetics*. 1999;Suppl 4:120-32.
16. van Krevelen DW, te Nijenhuis K. Properties of Polymers: Their Correlation with Chemical Structure; their Numerical Estimation and Prediction from Additive Group Contributions. Amsterdam, The Netherlands: Elsevier Science; 2009.
17. Hui YH. Handbook of Food Science, Technology, and Engineering. Abingdon, United Kingdom: Taylor & Francis; 2006.
18. Field SB, Franconi C. Physics and Technology of Hyperthermia. New York, USA: Springer Science; 2012.
19. Chik WW, Barry MA, Thavapalachandran S, Midekin C, Pouliopoulos J, Lim TW, Sivagangabalan G, Thomas SP, Ross DL, McEwan AL, Kovoov P, Thiagalingam A. High spatial resolution thermal mapping of radiofrequency ablation lesions using a novel thermochromic liquid crystal myocardial phantom. *J Cardiovasc Electrophysiol*. 2013;24:1278-86.
20. Wayne JG, Nath S, Haines DE. Microwave catheter ablation of myocardium in vitro. Assessment of the characteristics of tissue heating and injury. *Circulation*. 1994;89:2390-5.
21. Leertouwer TC, Gussenhoven EJ, van Jaarsveld BC, van Overhagen H, Bom N, Man in 't Veld AJ. In-vitro validation, with histology, of intravascular ultrasound in renal arteries. *J Hypertens*. 1999;17:271-7.